

Atomistic modeling of materials behavior under conditions of rapid heating

- 1. disintegration of Al core-Al₂O₃ shell nanoparticles**
- 2. short-pulse laser interactions with layered metal targets**

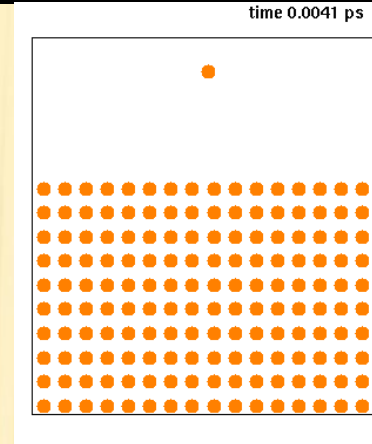
Chengping Wu, Leonid V. Zhigilei

Introduction to Molecular Dynamics (MD)

Molecular dynamics: computer simulation of the time evolution of a system of interacting particles by solving a set of classical equations of motion for all particles in the system.

$$m_i \frac{d^2 \vec{r}_i}{dt^2} = \vec{F}_i \quad i = 1, \dots, N$$

$$\vec{F}_i = -\nabla_i U(\vec{r}_1, \vec{r}_2, \dots, \vec{r}_N)$$



Input: interatomic interaction

$U(\vec{r}_1, \vec{r}_2, \dots, \vec{r}_N)$: description of thermal and mechanical properties of particular system

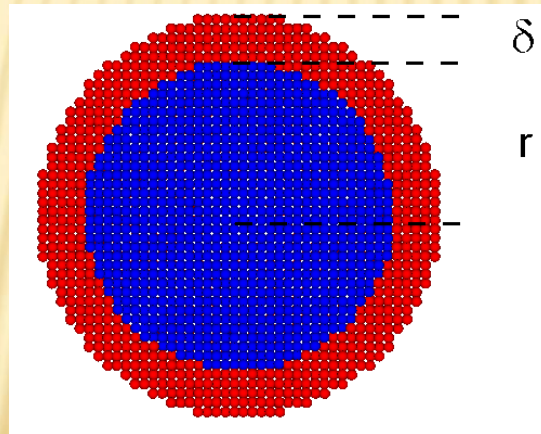
Output: evolution of the system

positions and velocities of all the atoms as a function of time, $\vec{r}_i(t), \vec{v}_i(t)$

Advantages of MD:

- **Simple**: solving a set of classical equations of motion
- **Basic**: making no assumptions about the processes/mechanism to be investigated
- **Atomistic view**: providing a detailed molecular/atomic-level information

Atomistic modeling of thermal and mechanical behavior
of aluminum core/alumina shell nanoparticles under
conditions of rapid heating



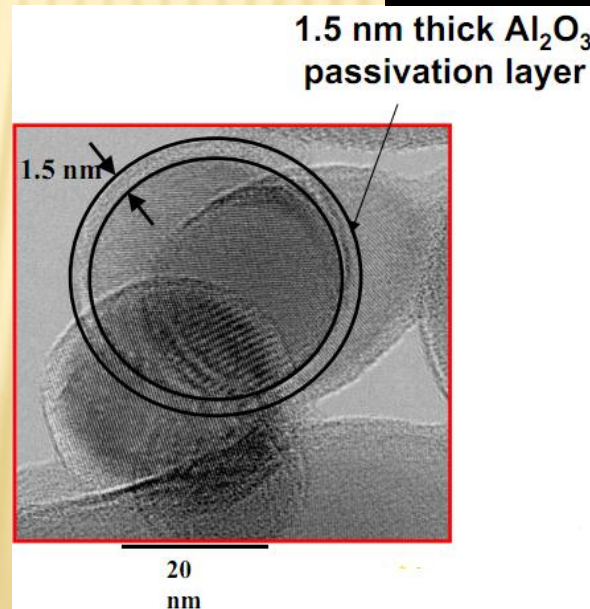
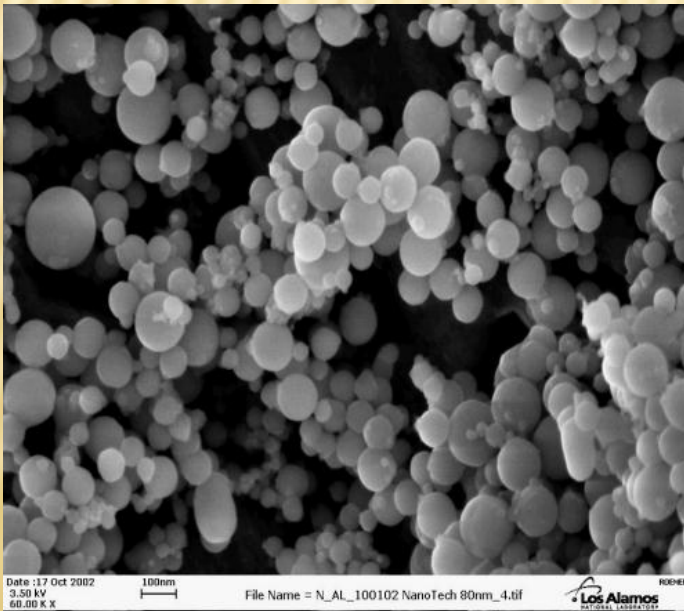
Motivation

Nano-thermite: mixture of nano-metallic (Al) particles (covered by a thin oxide shell, Al_2O_3) with some oxidizers, highly exothermic reaction after ignition, generally developed for military use, propellants, explosives, and pyrotechnics

compared with micro-thermite:

- Highly increased reaction rate
(increased by several orders of magnitude)
- Highly increased energy release rate
- Rapid heating during reaction 10^8 K/s

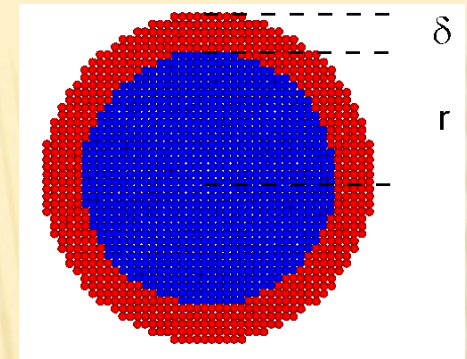
Transmission Electron Microscopy (TEM) image:



Todd M. Allen, et al

Motivation

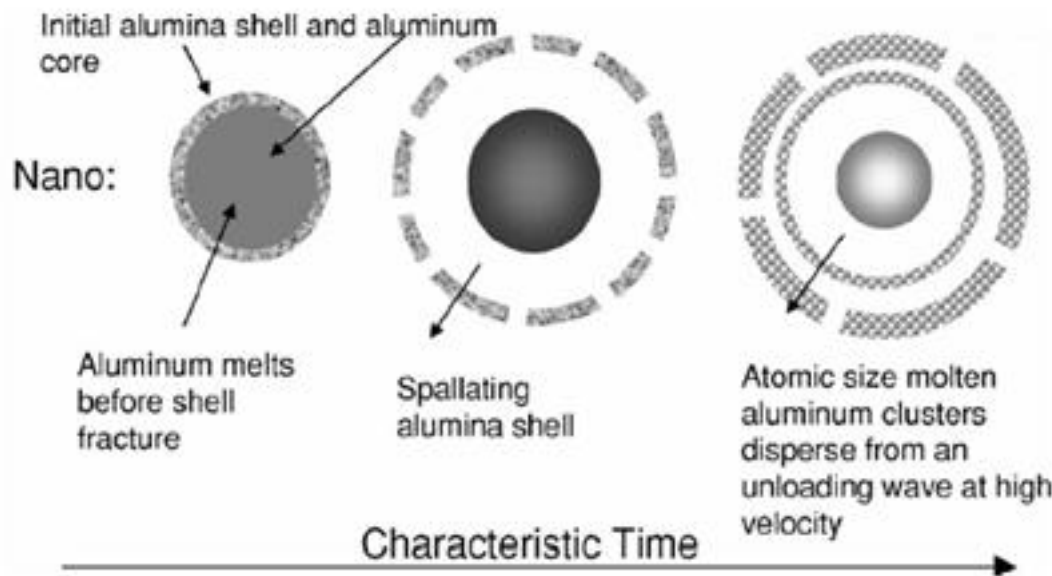
- **For Micron-size aluminum core/alumina shell particles,** their combustion (oxidation) can be explained by diffusion reaction mechanism (diffusion of the oxidizer to the metal or metal toward oxidizer)



- **For aluminum core particles,** their reactivity are increased by a magnitude. (Flame rates of 0.9-1 km/s compared to the order of centimeters or meters per second).

Diffusion mechanism

- **Theoretically, melt-dispersion mechanism is proposed**



Fast heating, core melting

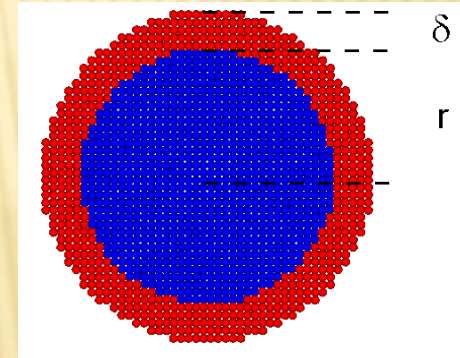
High compressive pressure in core, large tensile stress in shell

Fracture and spallation of shell

Molten core dispersion through spallation

Computational model

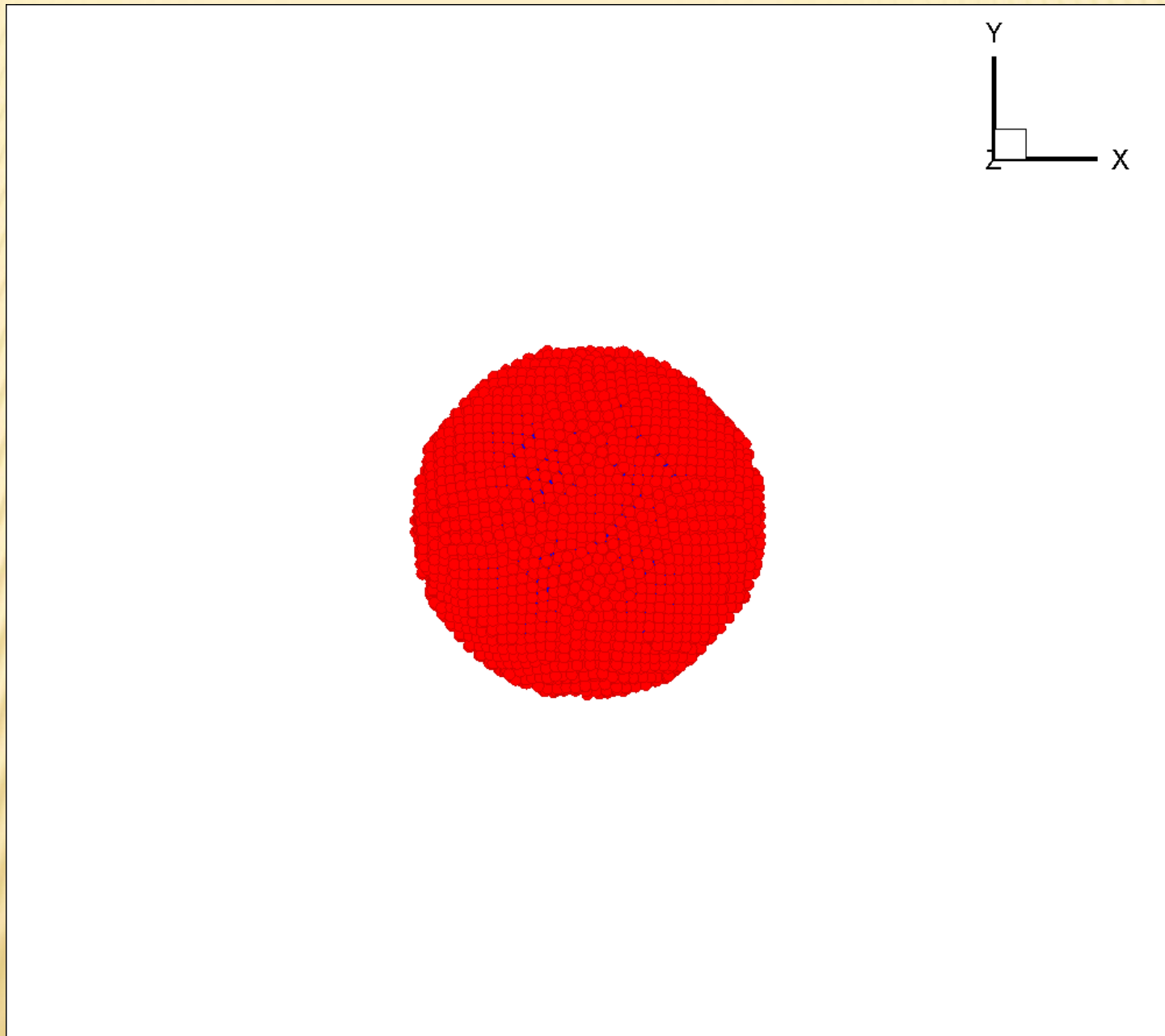
- **“Alumina” shell: pair potential** fitted to elastic modulus
 $B=234.8\text{ GPa}$, $G=141\text{ GPa}$, and $a=4.0817\text{ \AA}$. Shell has FCC crystal structure.
- **Aluminum core: Johnson’s EAM potential** fitted to cohesive energy, unrelaxed vacancy formation energy, atomic volume, elastic modulus, $B=96.6\text{ GPa}$, $G=30.3\text{ GPa}$, $a=4.0817\text{ \AA}$.
[Zhou, Wadley, Johnson, et al. Acta Mater. 49, 4005, 2001]
- **Al-Alumina interaction: pair potential** fitted to work of separation between Al and “Alumina”, $W_{\text{ad}}=1\text{ J/m}^2$
- **Heating rate:** $\sim 10^{13}\text{ K/s}$ – high, but **sufficient for mechanical relaxation during heating**



- ✓ Good description of elastic properties
- ✓ Overestimate both thermal expansion coefficients, but keep their ratio with error of 5%
- ✓ Underestimate volume change upon melting for Al, 4.0% compared with 6-7%

My computational model provide a semi-quantitative description of this core-shell system

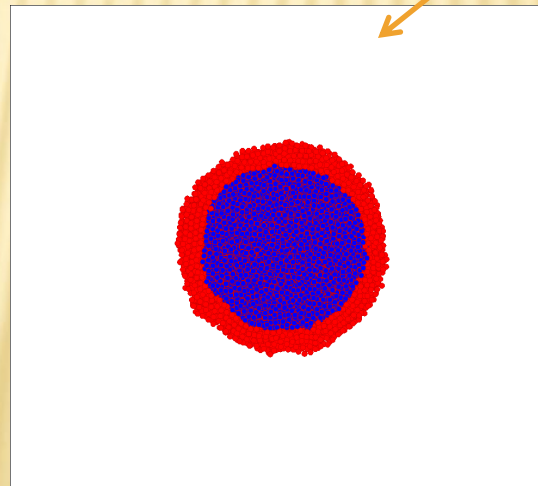
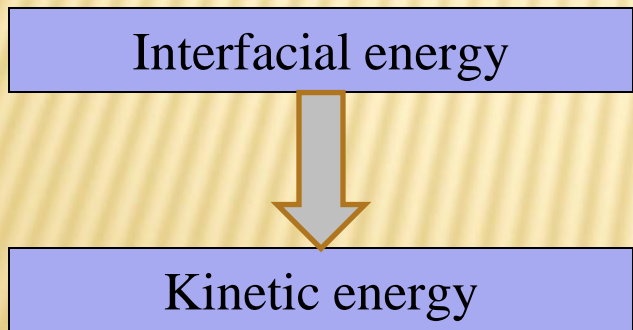
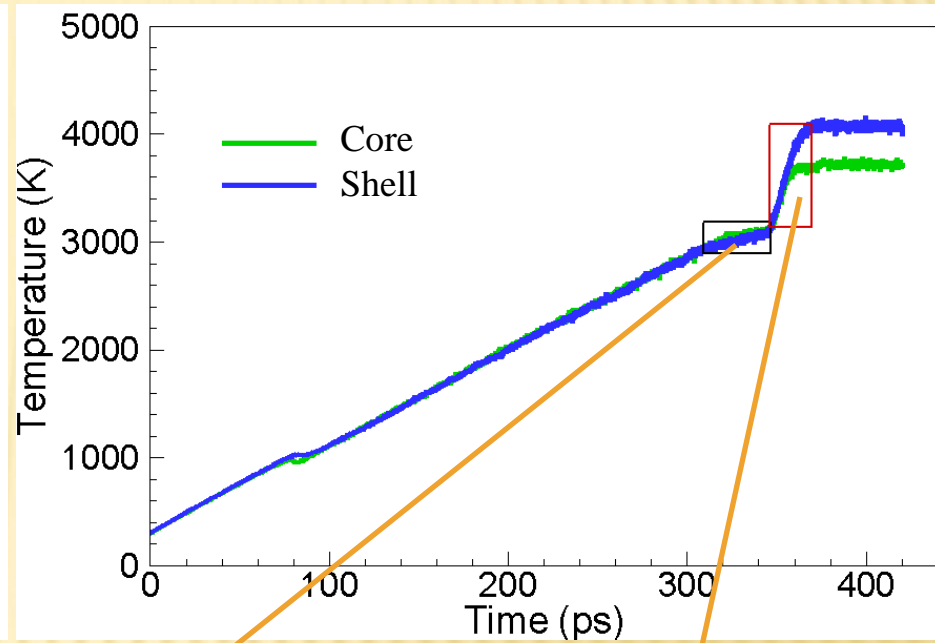
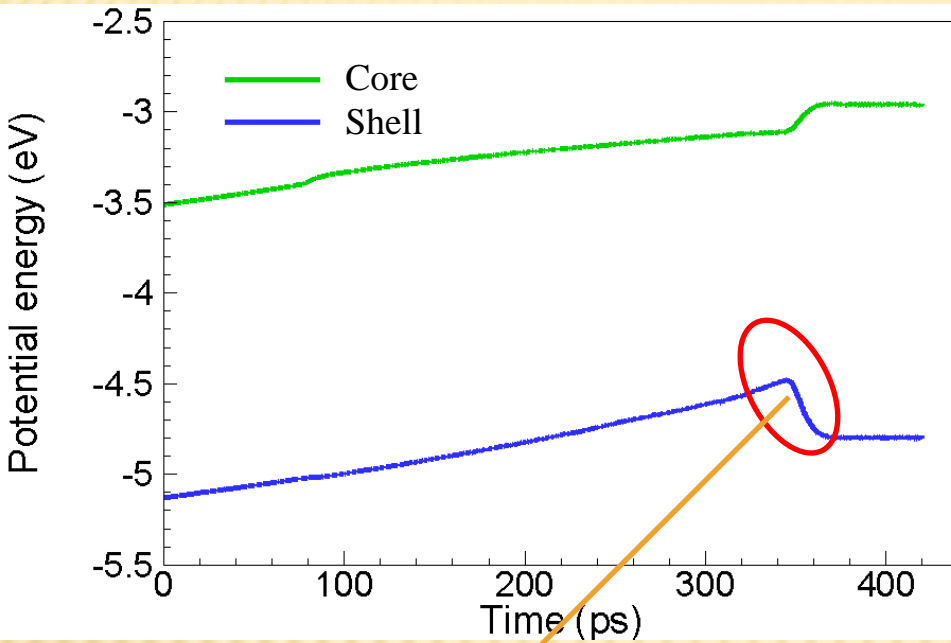
Jet-like ejection of the melted Al



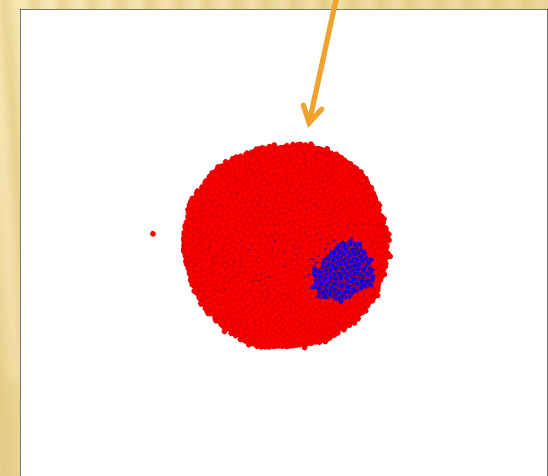
$r = 3.5 \text{ nm}$, $d = 0.5 \text{ nm}$ (10504 Al atoms, 5200 alumina atoms)

Mechanisms of Al ejection

$r=3.5$ nm, $d=1.0$ nm (Al:10504, Alumina:11952)

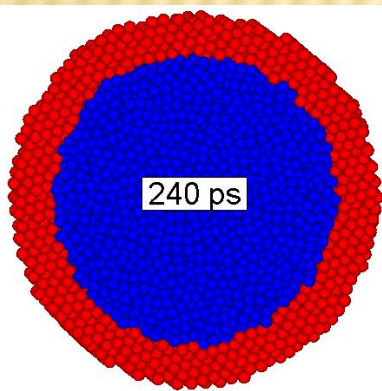
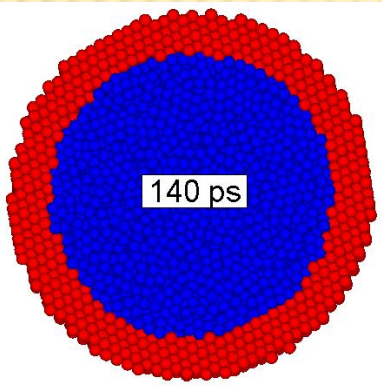
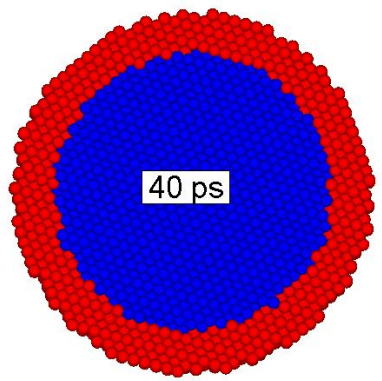


Localized thinning

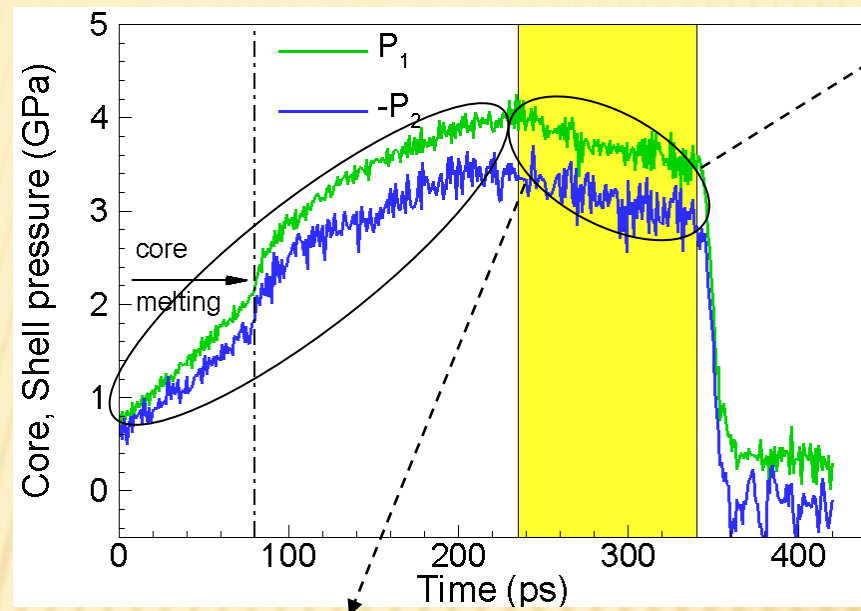


Ejection

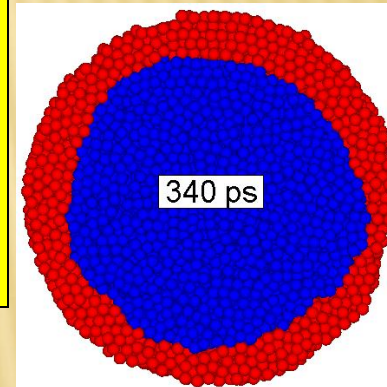
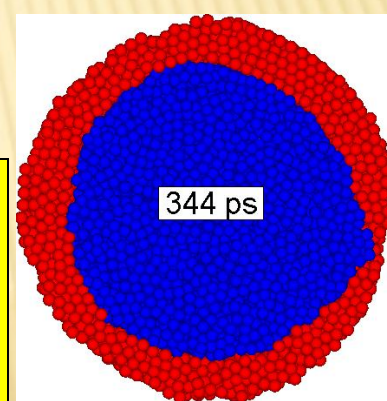
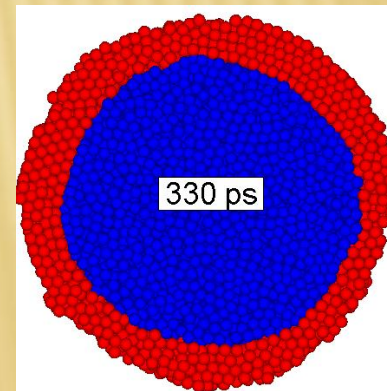
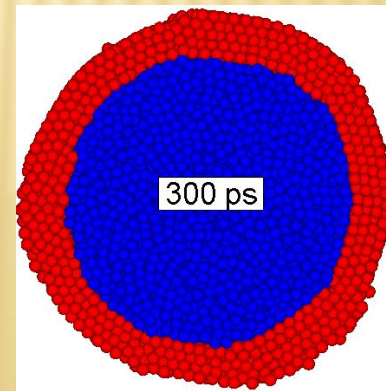
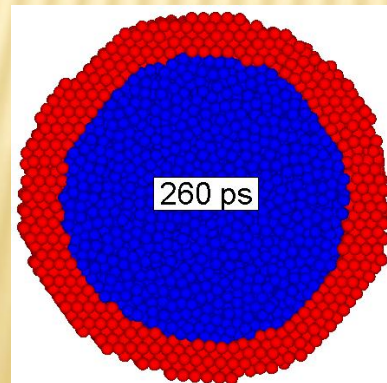
Elastic deformation \rightarrow Plastic deformation \rightarrow Thinning \rightarrow Ejection



Elastic deformation

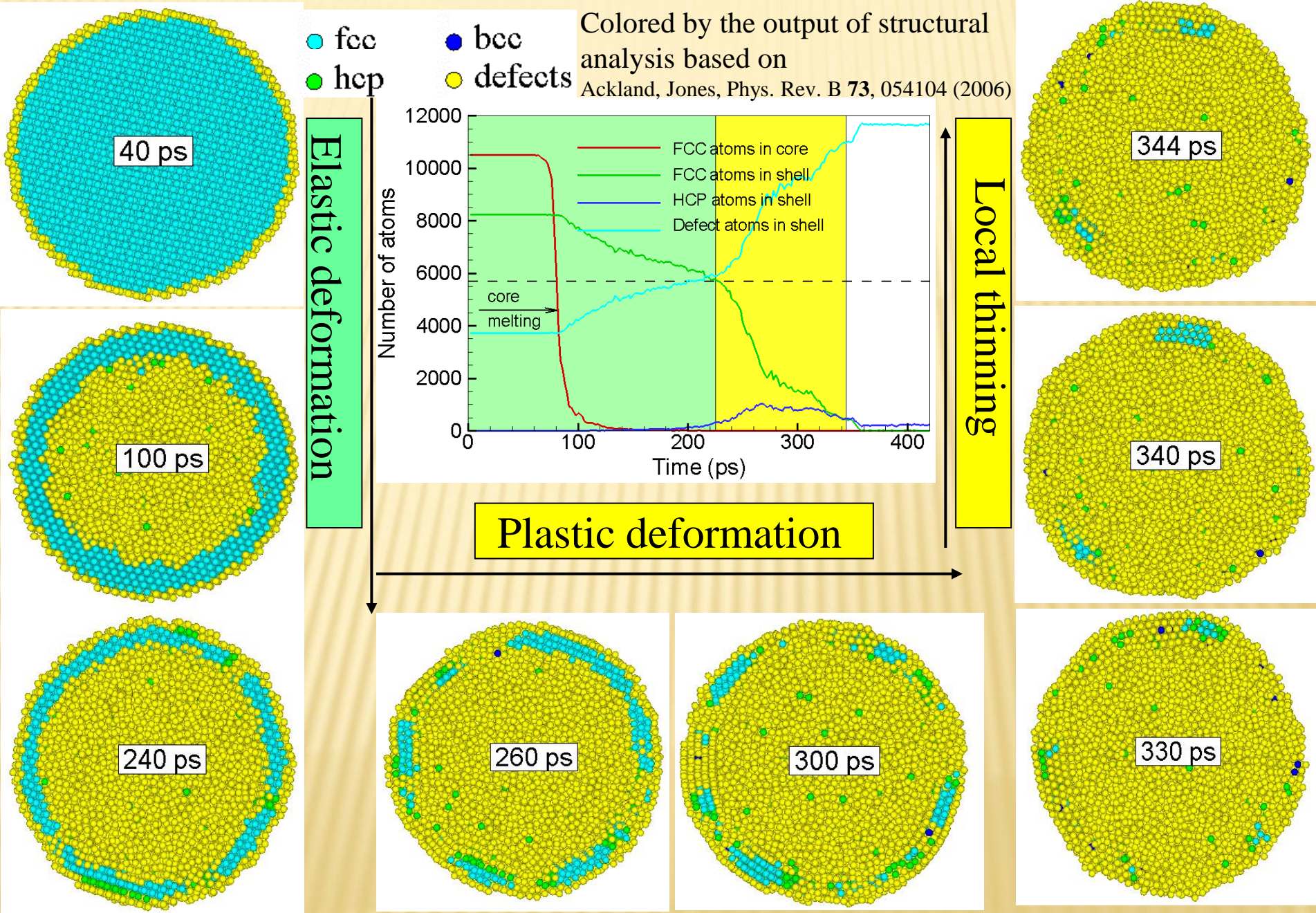


Plastic deformation



Local thinning

Elastic deformation → Plastic deformation → thinning → Ejection



Cluster analysis

	cluster	Number of atoms	Velocity(m/s)	Temperature(K)
r=3.5nm d=0.5nm	shell	5260	135.8	3561.1
	core	10444	102.26	1992.9
r=3.5nm d=1.0nm	Shell	12072	277.3	3942.1
	Core	10259	477.4	3456.3
	core	99	112.6	3194.7
r=3.5nm d=1.5nm	shell	21107	113.6	3907.3
	core	9568	370.1	3775.1

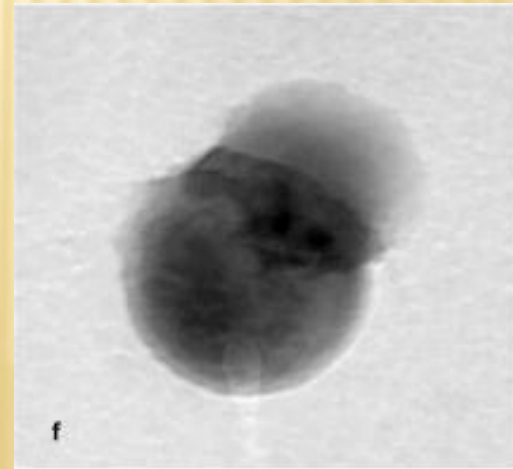
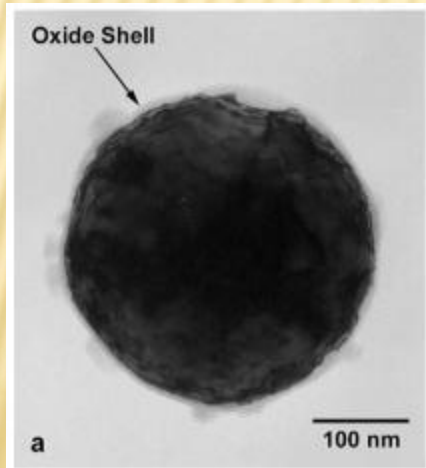
Ejected melt has a very high velocity on the scale of ~300 m/s → fast reaction of Aluminum nano-particle with surrounding oxidizers

Experimental proof of my result

In-situ transmission electron microscopy investigation of stress-relief mechanisms during melting of sub-micrometer Al-Si alloy particles



“plastic deformation of the thin oxide shell at temperatures around 823K to relieve the high stress generated by the expanding liquid during melting and heating, while the remaining oxides crack and eject liquid Al-Si, due to the internal pressure.”



Conclusions-on Al-Alumina nanoparticle

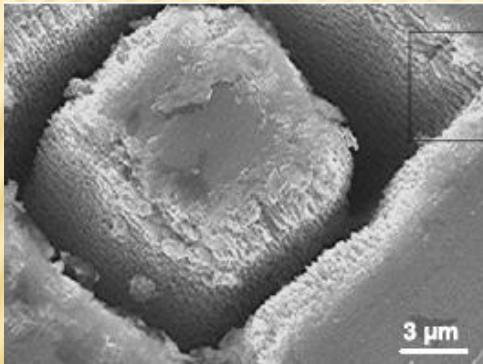
- Good semi-quantitative agreement with the melt dispersion mechanism: due to large difference in thermal expansion coefficient of Al and Alumina, heating and melting of the core create large compressive pressure in core and tensile stresses in the shell, which leads to the fracture of the shell
- Different from the melt dispersion mechanism, localized jet-like ejection of the melt is predicted from MD simulation, and 4 stages have been identified:

- Initial stage: alumina shell remains solid crystal and undergoes elastic deformation
- Second stage: when compressive pressure in core increases up to $\sim 4\text{GPa}$, the shell starts deform plastically to partially relax the core pressure
- Third stage: plastic deformation leads to localized thinning
- Final stage: fracture of the shell and ejection of the Al melt with very high velocity

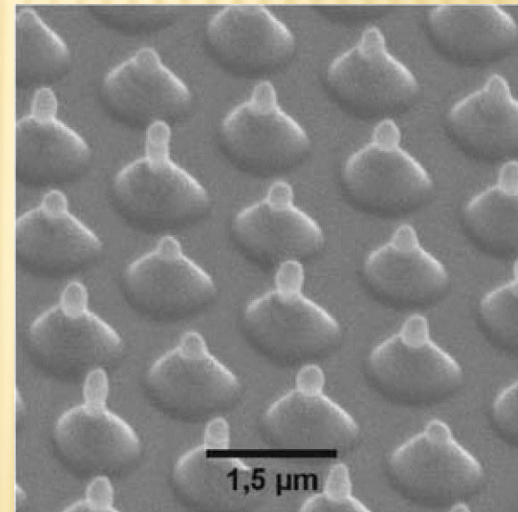
- This 4 stages are consistent with the results obtained by in-situ heating of Al-Si/alumina nanoparticles in a transmission electron microscope
- The ejected melt has a very high velocity of $\sim 300\text{ m/s}$, which may explain the high reaction rate between Al nano-particle and its surrounding oxidizers.

Introduction

Short-pulse laser-metal interaction: a subject of practical as well as fundamental scientific interest. It is in the core of many modern processing and fabrication techniques, like laser surface alloying, laser surface cleaning, laser notch formation and laser drilling.



Sanner et al., Appl. Phys. B **80**, 27, 2005



Korte, Koch, and Chichkov
Appl. Phys. A **79**, 879, 2004

Laser interaction with metals

Laser energy deposition-laser excitation of conduction band electrons



Relaxation/thermalization of the absorbed laser energy (*electron-phonon coupling, electron heat conduction*)



Conditions far from equilibrium---high-T/high-P region, ∇T , stresses, thermal and mechanical processes (*melting/resolidification, fracture/spallation, boiling, vaporization*)



Difficult to do experimental characterization and theoretical description of laser-induced structural changes, MD gives an alternative

Simulation Model of laser interaction with metals

**Physics missing
in classical MD:**

- Laser energy absorption by the conduction band electrons
- Electron-phonon equilibration and electronic heat conduction

Two-Temperature Model (TTM)—Continuum level

$$C_e(T_e) \frac{\partial T_e}{\partial t} = \nabla [K_e(T_e, T_l) \nabla T_e] - G(T_e)(T_e - T_l) + S(\vec{r}, t) \quad \text{Electronic temperature}$$
$$C_l(T_l) \frac{\partial T_l}{\partial t} = G(T_e)(T_e - T_l) \quad \text{Lattice temperature}$$

Advantages of TTM:

- Laser energy absorption by the conduction band electrons
- Electron-phonon equilibration and electronic heat conduction

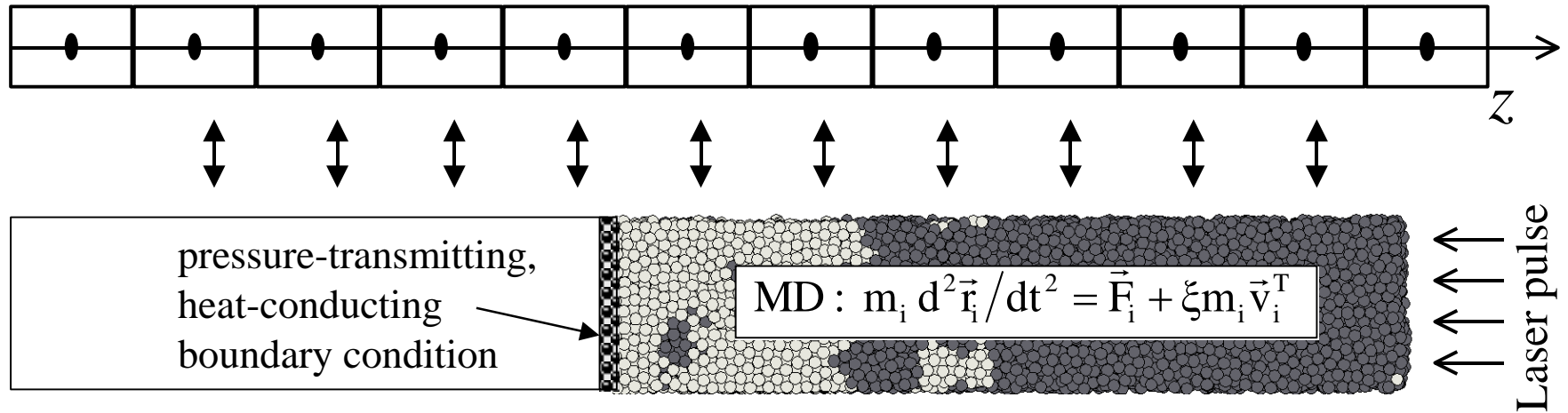
Disadvantages of TTM:

- Atomistic picture missing

Simulation model of laser interaction with metals

Combined atomistic-continuum (TTM-MD model):

$$C_e(T_e) \frac{\partial T_e}{\partial t} = \frac{\partial}{\partial z} \left(K_e(T_e, T_l) \frac{\partial T_e}{\partial z} \right) - G(T_e - T_l) + S(z, t)$$



$$C_l(T_l) \frac{\partial T_l}{\partial t} = G(T_e - T_l)$$

$$T_l^{\text{cell}} = \sum_{i=1}^{N^{\text{cell}}} m_i \left(\vec{v}_i^T \right)^2 / (3k_B N^{\text{cell}})$$

D. S. Ivanov and L. V. Zhigilei, *Phys. Rev. B* **68**, 064114, 2003

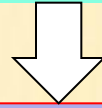
E. Leveugle, D. S. Ivanov, and L. V. Zhigilei, *Appl. Phys. A* **79**, 1643-1655, 2004

Laser-metal interaction physics included, atomistic picture will also be provided

Atomistic simulation of atomic mixing and structural transformations in **Ag film-Cu substrate system** irradiated by femtosecond laser pulse

Motivation of this research

Strong nonequilibrium (thermodynamic, electronic, mechanical) can be induced by short-pulse laser irradiation



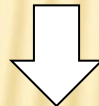
What will happen when short-pulse laser is applied on **layered targets**?

How the melting and resolidification happen?

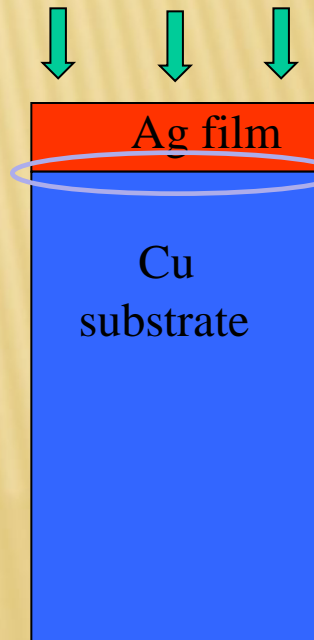
How do atoms mix for immiscible systems (like Ag-Cu)?

What structure will be generated at the interface?

???,etc



Atomic-level computer simulation → detailed information on the complex structural and phase transformations induced by short pulse laser irradiation



Computation model

➤ TTM (Two-Temperature Model)-MD (Molecular Dynamics)

D.S. Ivanov, L.V. Zhigilei, Phys.Rev.B 68 (2003) 064114

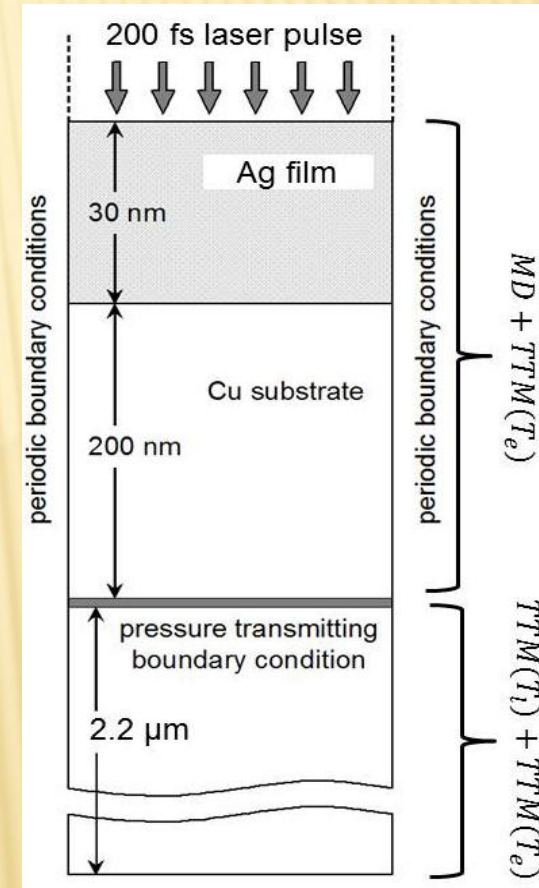
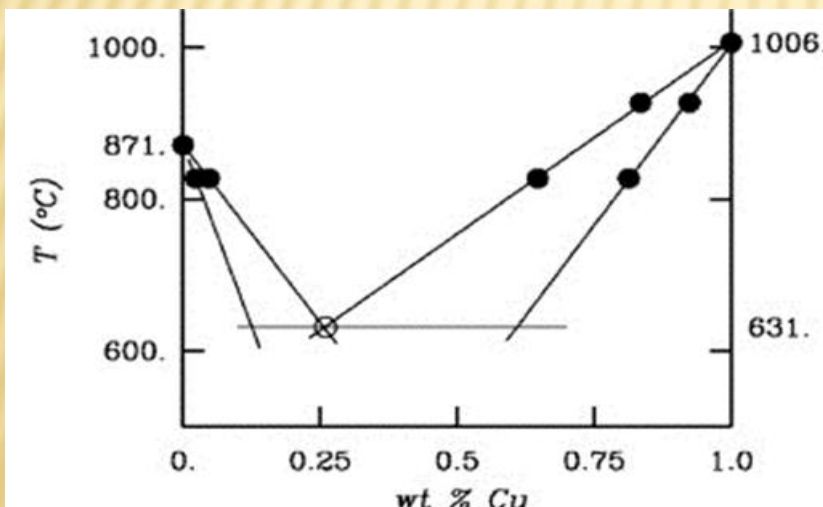
$$m_i \frac{d^2 \vec{r}_i}{dt^2} = \vec{F}_i + \varepsilon m_i V_i^T, \quad MD$$

$$C_e(T_e) \frac{\partial T_e}{\partial t} = \frac{\partial}{\partial z} \left(K_e(T_e) \frac{\partial T_e}{\partial z} \right) - G(T_e - T_l) + \text{Laser energy deposition}, \quad TTM(T_e)$$

$$C_l(T_l) \frac{\partial T_l}{\partial t} = G(T_e - T_l), \quad TTM(T_l)$$

continuum-level description of the laser excitation and subsequent relaxation of the conduction band electrons

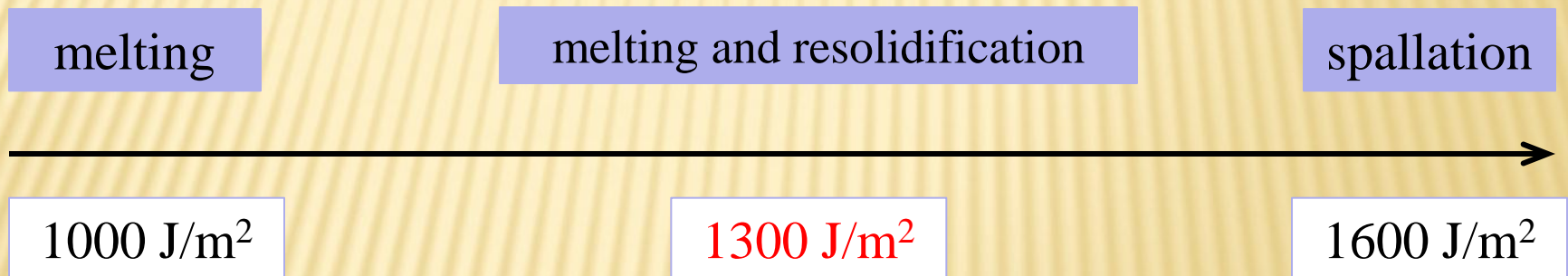
➤ EAM interatomic potential [Foiles, Baskes, Daw, PRB 33 (1986) 7983]



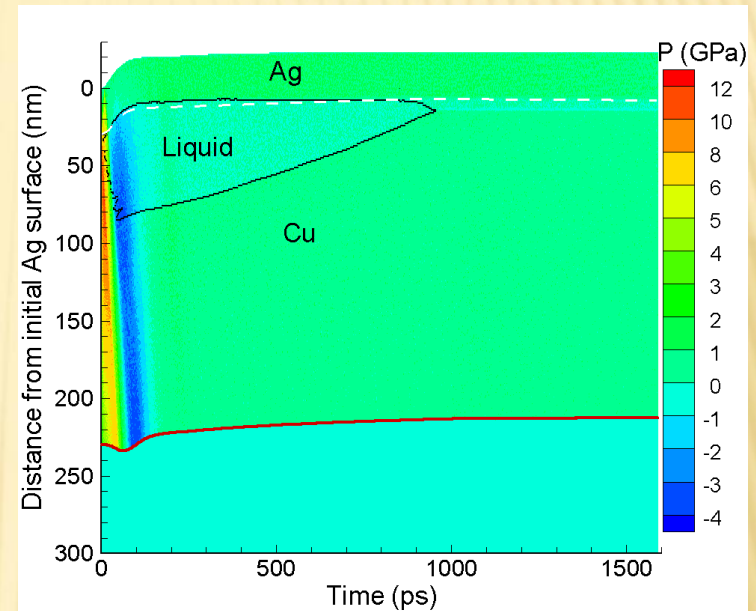
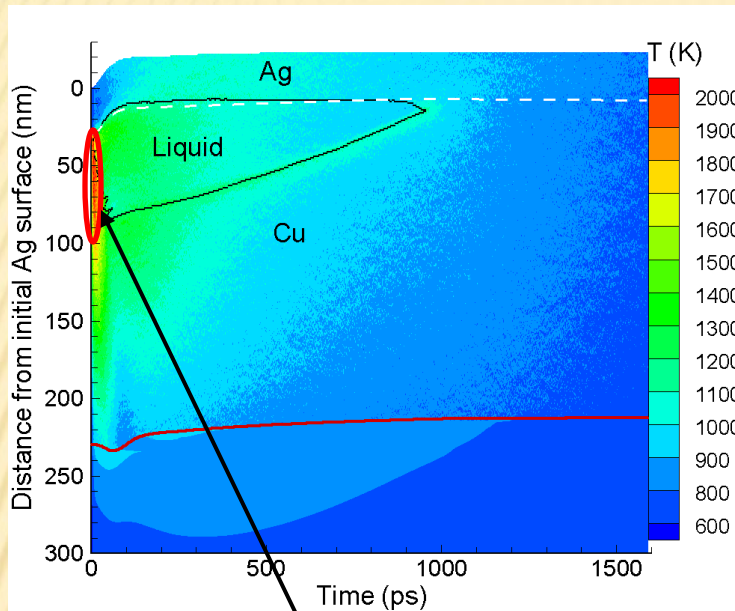
The potential gives good description of Ag-Cu system, the calculated phase diagram agrees semi-quantitatively with experiment

Webb III et al., Acta Mater. **53**, 3163, 2005

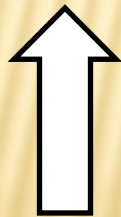
Simulation results and discussions



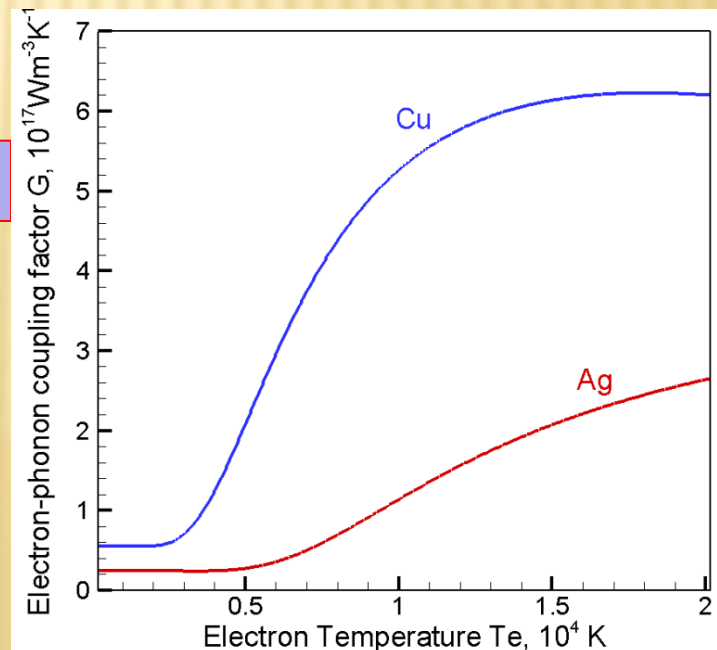
Simulation results and discussion – preferential sub-surface heating and melting



preferential heating and melting of Cu substrate

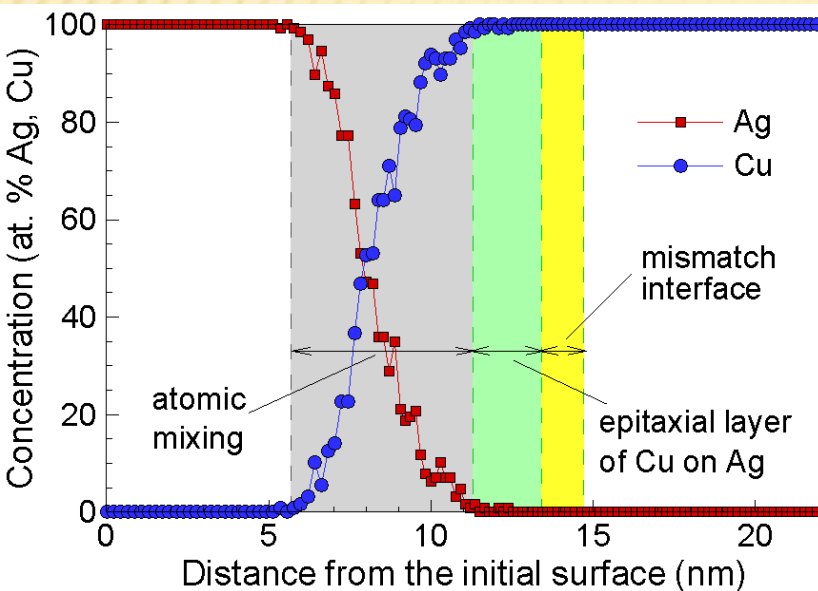
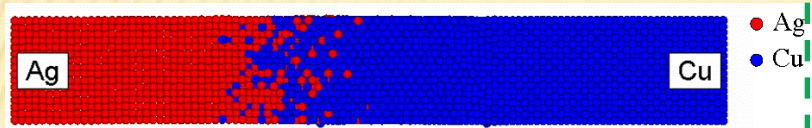


Stronger e-ph coupling of Cu



Simulation results and discussions – wider atomic mixing

Laser atomic mixing

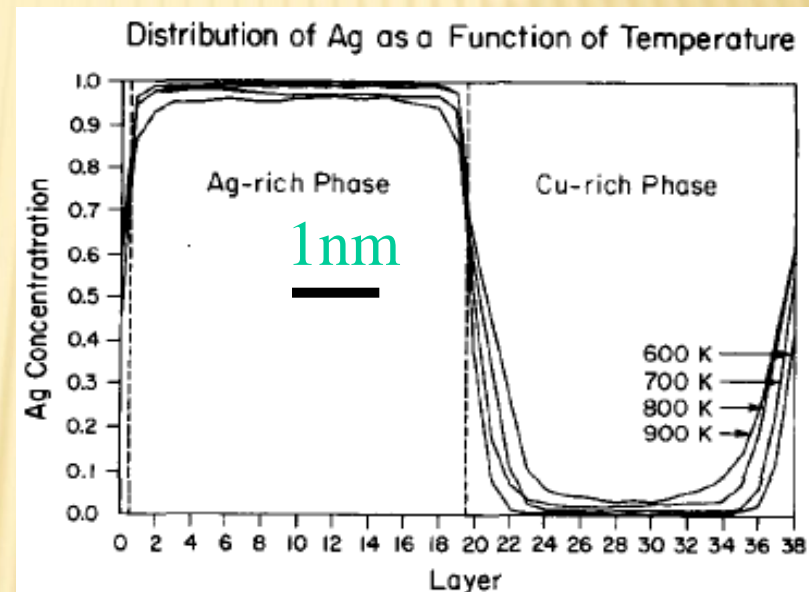


Equilibrium mixing

Monte Carlo simulation of Cu-Ag (001) interface

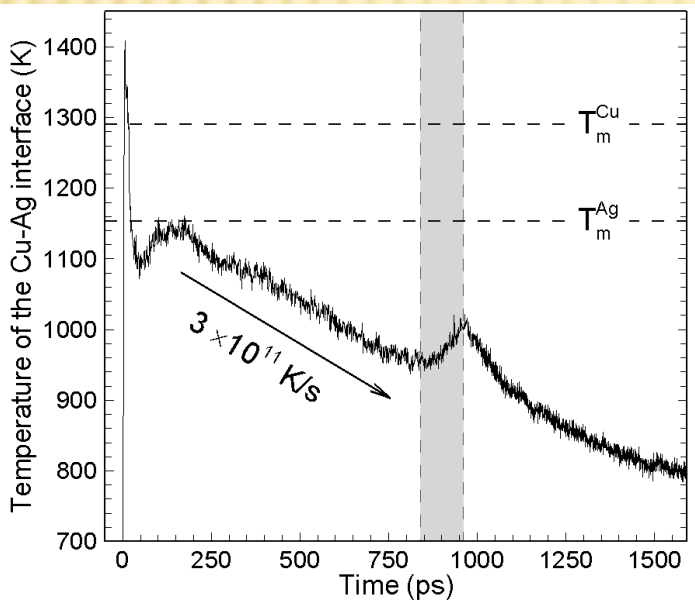
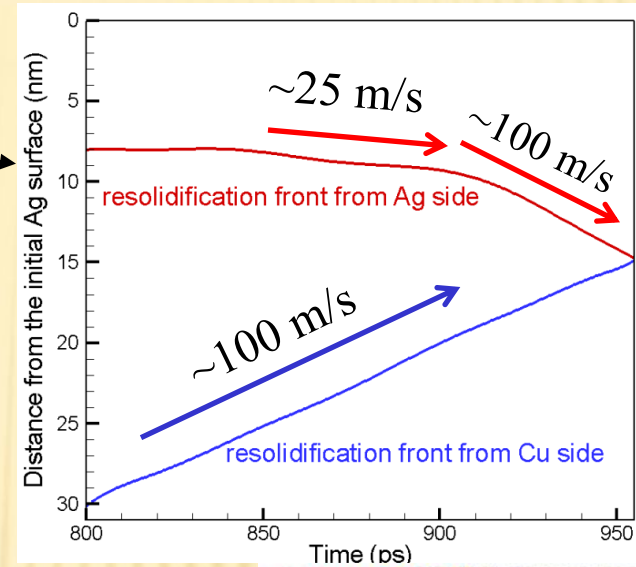
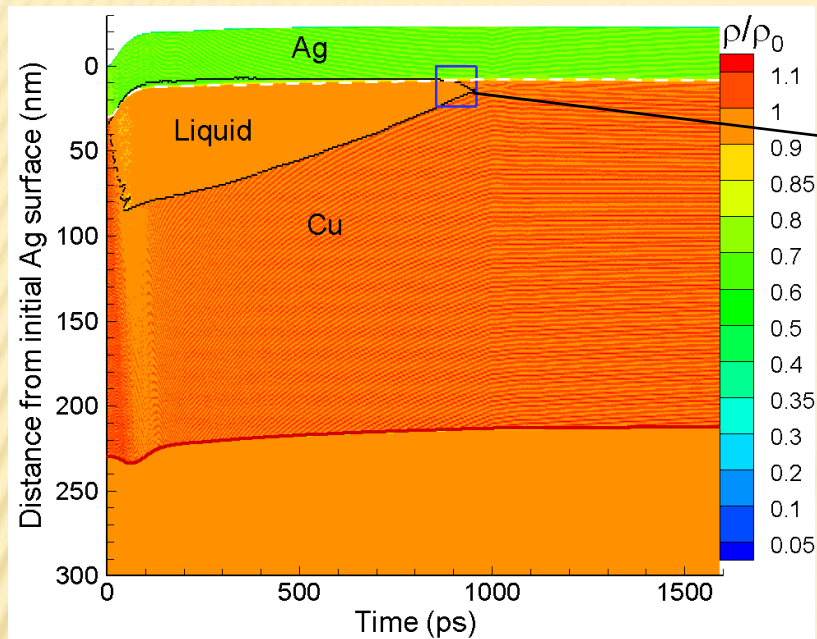
[Rogers III, Wynblatt, Foiles, Baskes,

Acta Metall. Mater. 38 (1990) 177]



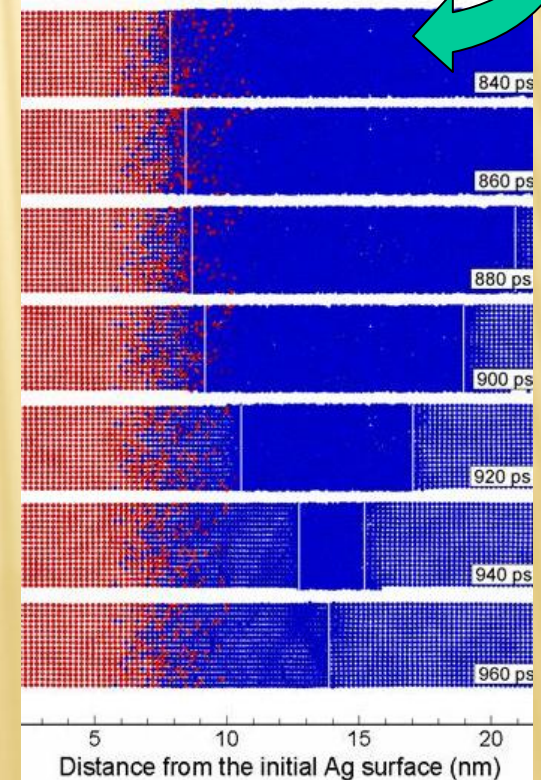
Laser atomic mixing >> mixing at equilibrium configuration

Simulation results and discussion - epitaxial growth of Cu on Ag

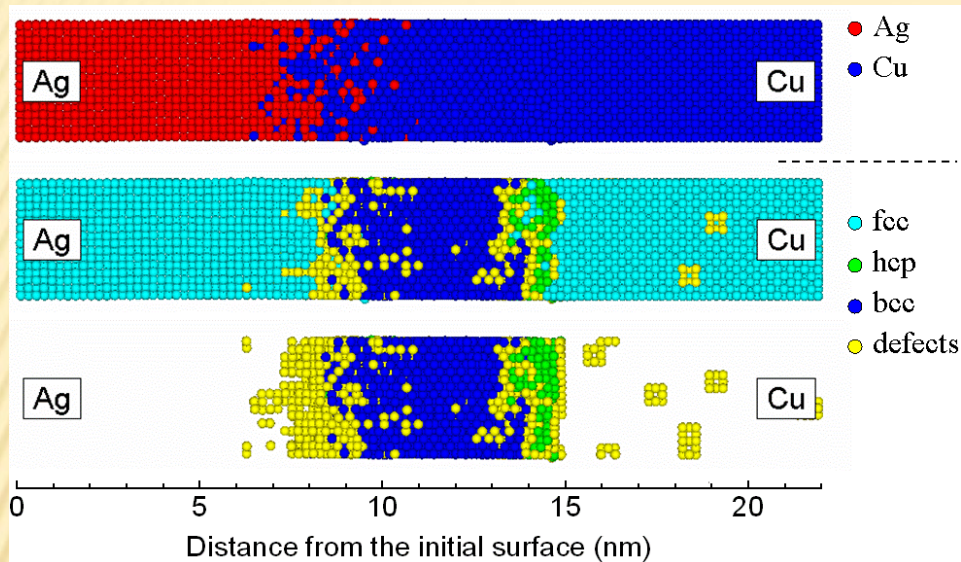


Strong undercooling

epitaxial growth of Cu on top of Ag

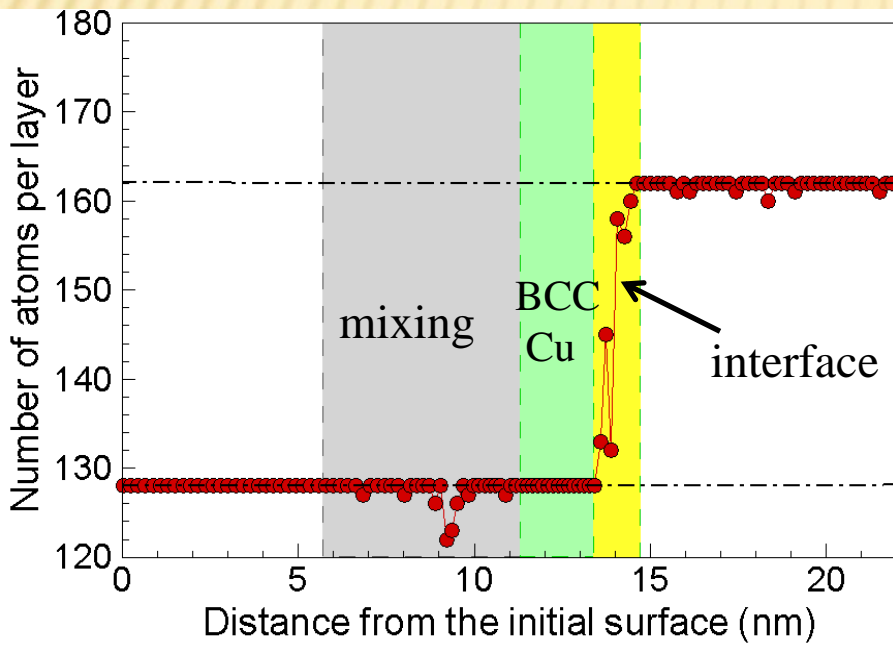


Simulation results and discussions – structure of resolidified region



Atomic configurations at 1.59 ns after laser pulse.

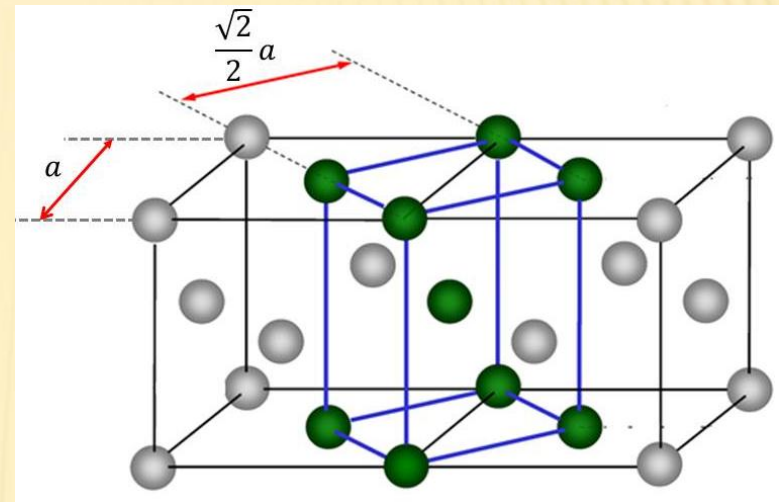
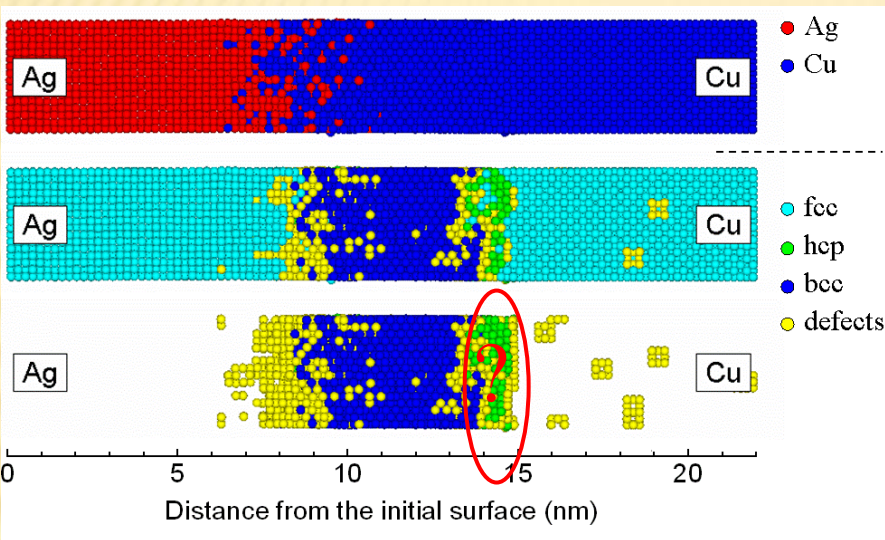
Colored by the output of structural analysis based on Ackland, Jones, Phys. Rev. B **73**, 054104 (2006)



Due to epitaxial growth of Cu on top of Ag, 2 nm wide BCC Cu layer is generated

The new lattice mismatch interface is separated from atomic mixing region by the intermediate BCC Cu layer

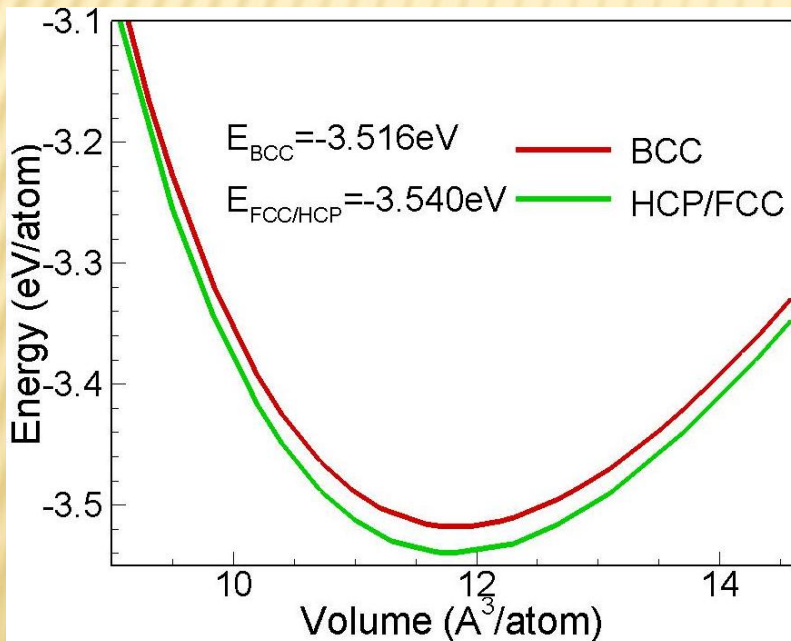
Simulation results and discussions – BCC Cu layer



Good match between the lattice parameter of BCC Cu structure and the 1st-neighbor distance in the FCC Ag structure:

BCC Cu: $a \sim 2.90 \text{ \AA}$

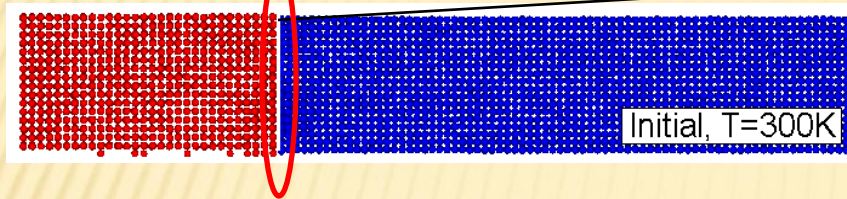
FCC Ag: 1st neighbor distance = $\frac{\sqrt{2}}{2} a \sim 2.89 \text{ \AA}$



Small energy difference of BCC Cu & FCC Cu:
The difference in the cohesive energies between BCC Cu and FCC Cu predicted with FBD EAM potential is small (22 meV/atom)

Simulation results and discussion – the runaway lattice-misfit interface

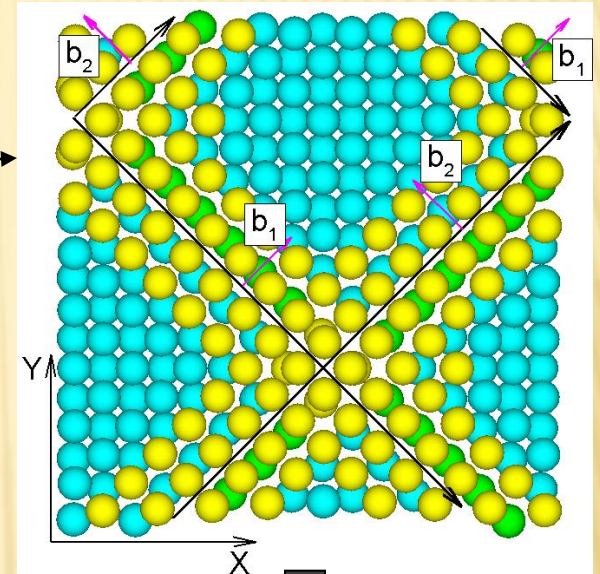
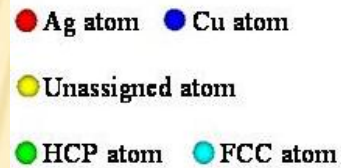
Initial system



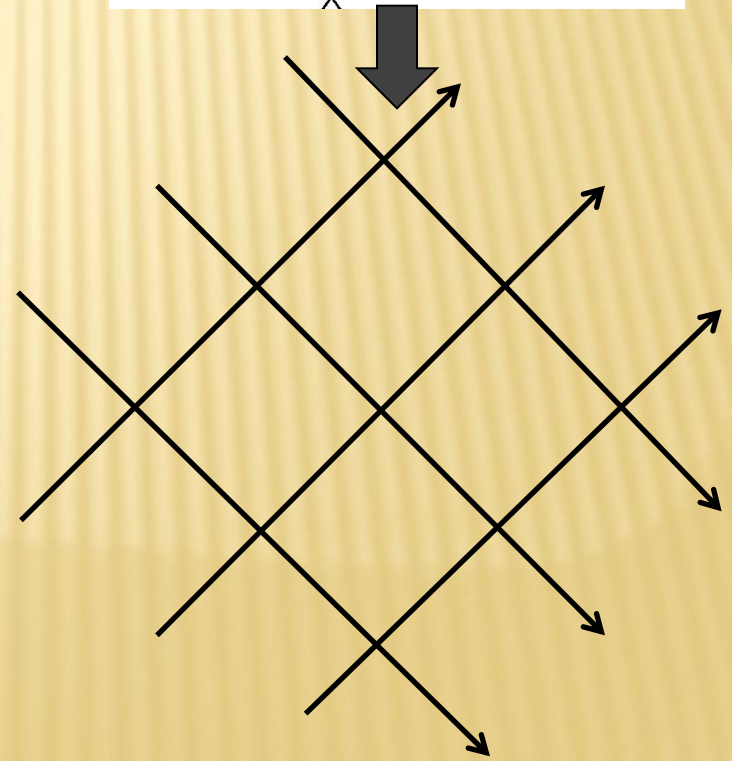
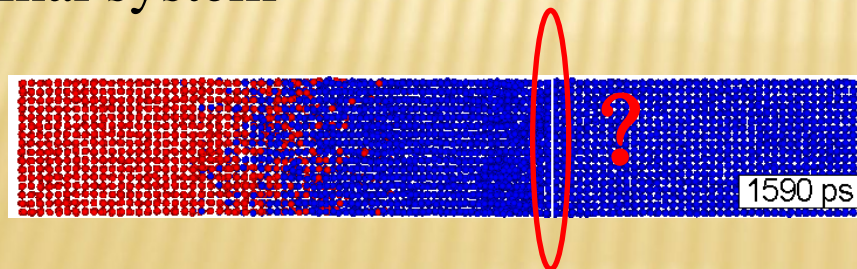
Misfit dislocation network
at the interface

$$\vec{b}_1 = \frac{1}{2} [1\ 1\ 0]$$

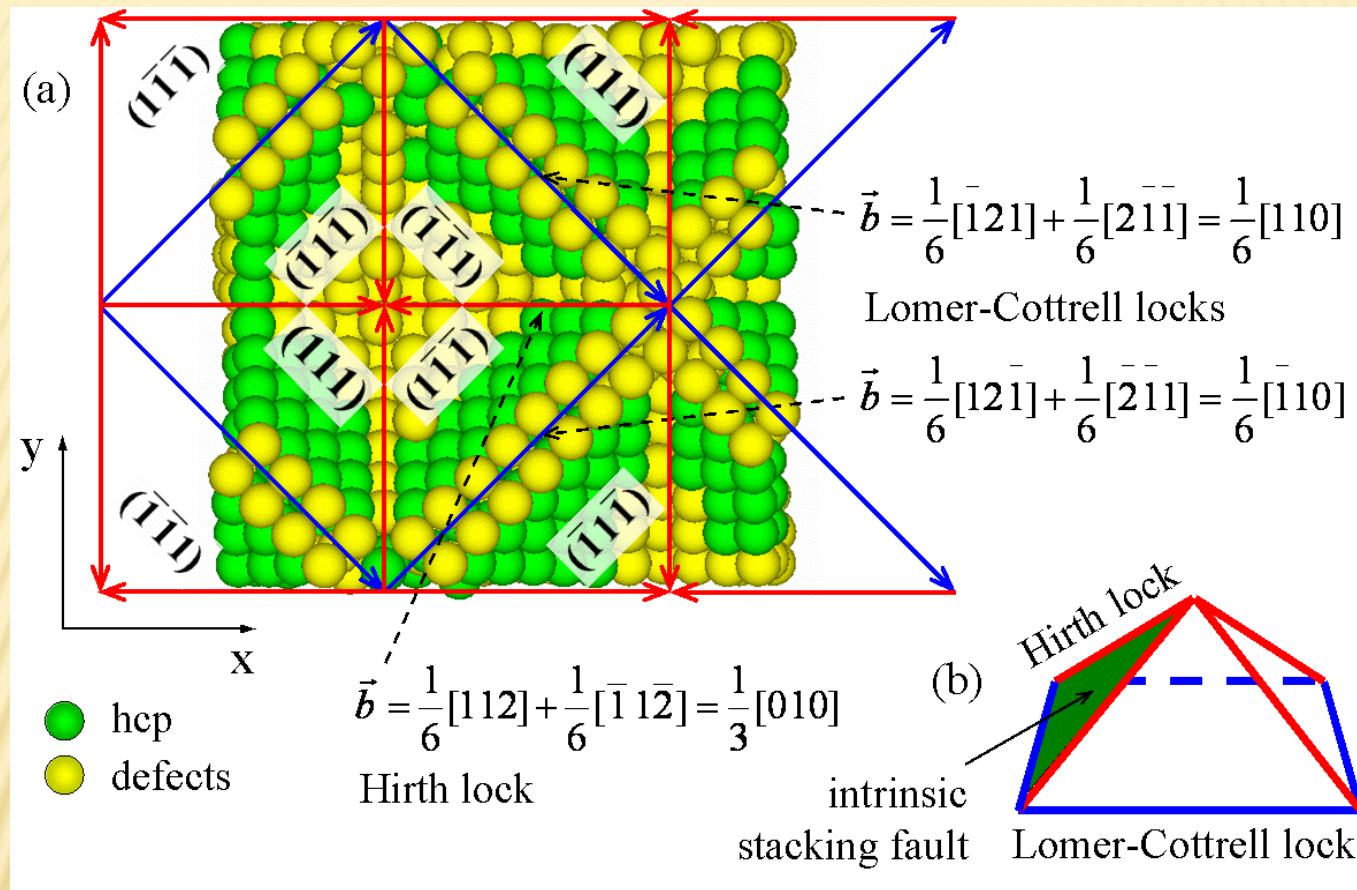
$$\vec{b}_2 = \frac{1}{2} [\bar{1}\ 1\ 0]$$



Final system



Simulation results and discussions - the runaway lattice-mismatched interface



The runaway mismatched interface: complex three-dimensional corrugated structure consisting of a periodic array of stacking fault pyramids outlined by stair-rod partial dislocations



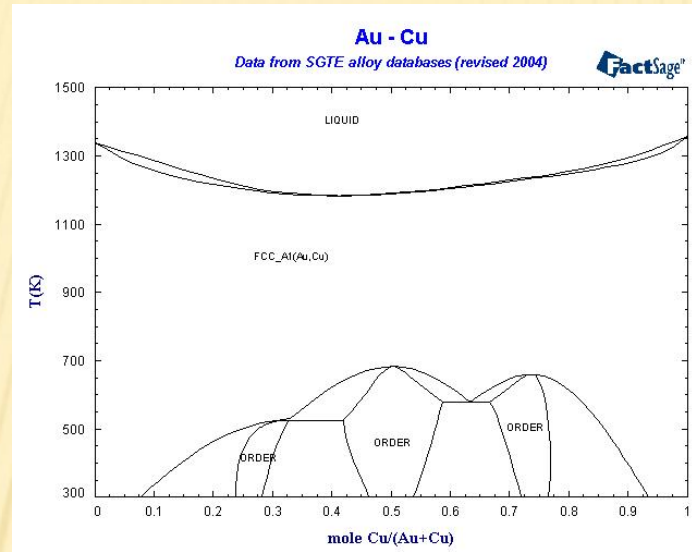
The runaway mismatched interface and BCC Cu layer: strong barrier for dislocation propagation, resulting in the effective hardening of the layered structure

Conclusions on Ag-Cu simulations

- Preferential sub-surface heating and melting of Cu substrate
- Much wider laser atomic mixing (~ 4 nm) than at equilibrium (< 1 nm)
- Due to strong undercooling, epitaxial growth of Cu on top of Ag is observed, leading to the generation of a thin film (~ 2 nm) of BCC Cu layer
- The runaway lattice-mismatch interface (between BCC Cu and FCC Cu) is found to have a complex 3-D corrugated structure consisting of a periodic array of stacking fault pyramids
- The laser-induced BCC Cu layer and 3-D runaway lattice-mismatch interface are likely to present a strong barrier for dislocation propagation, resulting in the effective hardening of the layered structure

Current and Future work

1: Femtosecond laser irradiation on Au film-Cu substrate (miscible) to compare with Ag-Cu



2: Femtosecond laser irradiation on Cu film-Ag substrate to compare with Ag film-Cu substrate

3: Femtosecond laser irradiation on Au film-Si substrate, relevant for semiconductor industry

4: Femtosecond laser ablation of Ag and Al, to compare with experiments conducted by Prof. Peter Balling's group in Denmark

Thanks for your attention!